IEEE Access
Multidisciplinary | Rapid Review | Open Access Journal

Received July 14, 2020, accepted August 29, 2020, date of publication September 18, 2020, date of current version September 29, 2020.

Digital Object Identifier 10.1109/ACCESS.2020.3024625

Developing Learning-Based Preprocessing Methods for Detecting Complicated Vehicle Licence Plates

MEERAS SALMAN AL-SHEMARRY[1,2] **AND YAN LI**[1]

[1]Faculty of Health, Engineering and Sciences, School of Sciences, University of Southern Queensland, Toowoomba, QLD 4350, Australia
[2]Department of Computer, College of Science, Karbala University, Karbala 56001, Iraq

Corresponding author: Meeras Salman Al-Shemarry (meerassalmanjuwad.al-shemarry@usq.edu.au)

This work was supported by University of Southern Queensland and the Ministry of Higher Education and Scientific Research of Iraq.

ABSTRACT A licence plate detection (LPD) system is an important tool in several roadway traffic applications. This study aims to develop an advanced detection system that works well in complicated scenarios. It proposes a robust preprocessing enhancement method for accurately detecting the licence plates from difficult vehicle images. The proposed method includes the combination of a Gaussian filter, an enhancement cumulative histogram equalization method, and a contrast-limited adaptive histogram equalization technique. The local binary pattern and median filter with histogram of oriented gradient descriptors are used as powerful tools to extract key features from three types of licence plate resolutions. The extracted features are used as input to support vector machine classifier. Processing methods, such as a position-based method are used with the detector to reduce unwanted bounding boxes, as well as false positive values. Four databases consisting of 2050 vehicle images under different conditions are used. Various detection metrics, object localization, and the receiver operating characteristic (ROC) curve are used to evaluate the performance of the proposed method. The experimental results on vehicles databases in several languages, including English, Chinese, and Arabic number plates, show that the proposed method has achieved significant performance improvements. It outperforms the state-of-the-art approaches in terms of both the detection rate and the processing time. The detection rate when trained with 1520 LP images is 99.62% with a false positive rate of 1.675% for complicated images. The average detection time per vehicle image is 0.2408 milliseconds.

INDEX TERMS Histogram of oriented gradient, licence plate detection, local binary patterns, support vector machine.

I. INTRODUCTION

Automatic number plate recognition (ANPR) systems have become a very important tool in many surveilling applications over the past few decades. They are often used as a surveillance technique to identify licence plates of vehicles and are very useful for security systems, highway road tolling systems, traffic sign systems, tracking, and parking management systems [1]–[5]. The existing systems often work under some standard conditions, such as low-high lighting, rain, and limited day-night lighting. It is still very challenging to identify licence plates (LPs) from complicated vehicle images because of environmental effects.

The associate editor coordinating the review of this manuscript and approving it for publication was Naveed Akhtar.

A robust licence plate detection (LPD) system is desirable to effectively work under all sorts of difficult conditions, such as night, dusk, rain, fog or snow; with images that are blurred, rotated, low-high lighting, distorted, with complex backgrounds and different colors. A number of examples for problematic licence plate (LP) images are shown in Fig. 1.

Some examples for ANPR applications are shown in Fig. 2. As an LPD system is rather difficult, the feature extraction techniques for doing this task should be developed carefully to extract and classify relevant features from regions of interest. Several extraction methods are widely used individually or combined together for the LP detection, such as local binary patterns (LBPs) [6], global and local features [7], Haar-like features [8], scale invariant feature

FIGURE 1. Examples for complicated images of an LP included in the databases.

FIGURE 2. Examples of ANPR applications.

transform (SIFT) [9], histogram of oriented gradient (HOG) [10], and so on.

The robustness and distinctiveness of the LBP descriptor is usually used to capture the important information that is sensitive to the illumination and rotation conditions [11]. But especially with distorted images, the descriptor needs to be further improved to focus on important information. Since the HOG focuses more on the edge information of an image, it is used widely to detect objects inside an image [10]. Therefore, the HOG features have been used with LBPs to obtain good extraction results. The main contributions of this study are:

1) Developing a new pre-processing method that includes the combination of a Gaussian filter, the enhancement cumulative histogram equalization (ECHE) method, and contrast-limited adaptive histogram equalization (CLAHE) technique to filter out unwanted LP regions to improve the accuracy of the detection system.
2) Improving the work of the HOG descriptor by using a median filter and combined it with the LBP descriptor to produce a powerful feature extraction method for complicated image environments, such as low/high contrast, fogginess, blurriness, rotated LPs, and dark, or complex backgrounds.
3) Increasing the classification accuracy by applying a support vector machine (SVM) and extreme learning machine (ELM) as an effective classifier, separately, with a new updated descriptor MHOG and LBP descriptor.
4) Removing redundant bounding boxes, which increase the false positive rate, using processing methods, such as a position-based method (mean-shift) with detectors.
5) Evaluating the proposed method using several performance measurement metrics and comparing its performance with the newest existing LPD methods.

This paper is organized as follows: Section II reviews the related research work. Section III introduces the proposed method, the details about the HOG and LBP descriptors, and the SVM and ELM classifiers. Section IV presents the databases. Section V shows the experimental results. Section VI presents the comparison with other existing methods. Finally, Section VII describes the conclusions and future work.

II. RELEVANT WORK

The main goal of developing an LPD system is to identify the licence plate number from the regions of interest (ROIs) in vehicle images. Many LPD methods in the literature were proposed. Although the LPD systems have been studied for many years, it is still very challenging to detect LPs from low quality images. Some methods developed depended on a specific color or language, or were limited to fine weather conditions, while others were sensitive to the lighting and complex backgrounds [12]–[14]. In addition, the angle of camera and the distance constraint make an LPD system less robust [15]. The detection of LPs in hazardous conditions is not easy, especially with complex backgrounds, which often produces a number of non-LP regions. For example, the proposed method by Azam and Islam [16] was not robust for angle invariant nor with distance. The texture-based methods are widely used by many researchers due to the significant texture change in the pixels greyscale level. The support vector machine (SVM) classifier is one of the supervised machine learning algorithms that is commonly used for classification and regression [17]. It can be seen as a type of single layer forward neural network (SLFN), called a support vector network [18]. The output be very good using a SVM if it is used to detect objects with good pre-processing and extraction techniques. The method by Kusakunniran, *et al.* [19] used a SVM as the machine learning tool, and fed the candidate license plate (CLP) images as the input to the SVM during the training and testing phases. In that study, the SVM was applied directly to the input images without any discriminative features being extracted. It made the detection system very sensitive to noise and geometric transformation. As a result, the detection accuracy was reduced to 80% and the training time was increased. Recently, deep neural networks (DNNs) [20] and convolutional neural networks (CNNs) [21] have been used as an automatic means to learn the key features in LPs. The DNN algorithms can combine the feature extraction and classification into one unified neural network framework. They have shown a higher detection accuracy. However, the features learning mechanism in DNNs cannot guarantee robustness in difficult image conditions, for example, rotation and scaling,

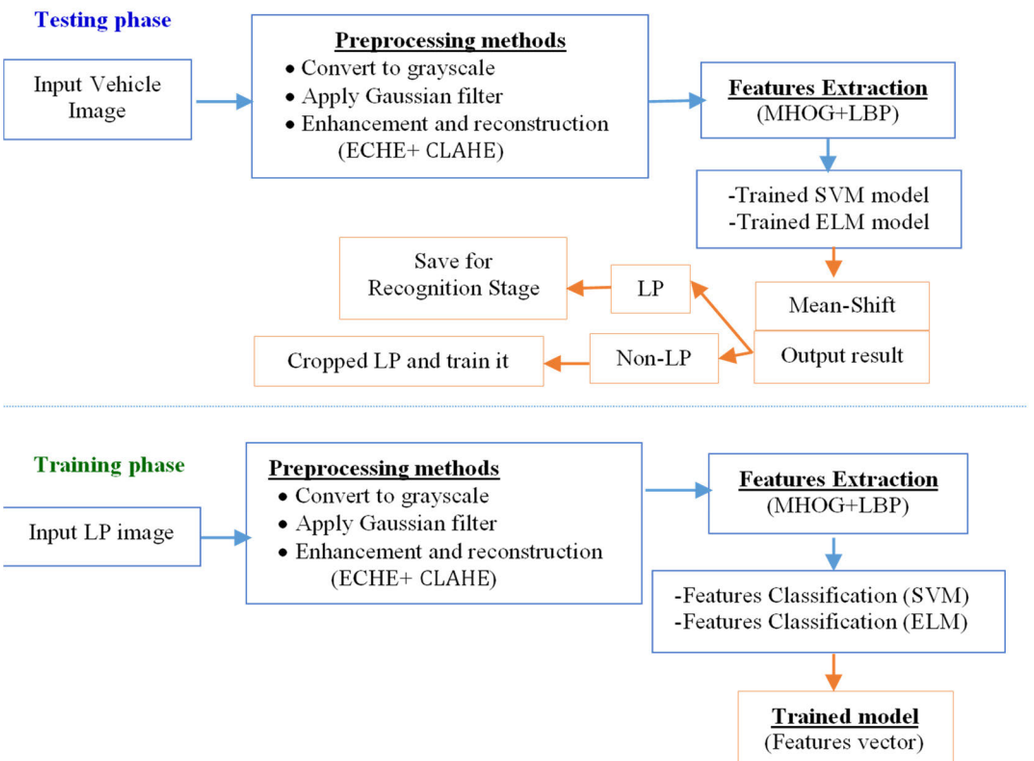

FIGURE 3. The structural diagram of the proposed LPD method for both testing and training phases.

unless the training samples can cover various observation conditions. Furthermore, their computational costs during both training and detection processes are expensive due to the multi-hidden-layer structure. In [22], a method using a CNN to learn features and an ELM as the classifier was reported. That method obtained competitive results with less computation time compared with those with DNN methods. However, the performances of those methods were compromised with the real conditions of a complex background and changing outdoor light conditions. Therefore, using a combination of textures features with good pre-processing methods to detect the LPs from complicated images can result in a better system performance. With the high speed of vehicles, not only the accuracy but also the computational speed are the key factors for real-time applications.

This paper proposes an efficient framework for improving the performance of an LPD system. It includes a pre-processing method, containing a Gaussian filter, enhancement cumulative histogram equalization (ECHE) and contrast-limited adaptive histogram equalization (CLAHE) methods. This combination works well for all conditions, and is suitable for different LP colors, styles, and languages. It can be applied to enhance any existing ANPR system with different databases. After the pre-processing stage, this study employs two powerful descriptors, HOG and LBP [23], [24]. A median filter was used with HOG (MHOG), descriptor to reduce noise during the extraction stage. The MHOG and LBP descriptors are used to extract several significant features from LP images. Finally, the SVM is used to build the trained model to detect the LP regions and also an ELM classifier was used for evaluation purposes. An English car database which was reported by Al-Shemarry *et al.* [25] was used in this study. This database contains many complicated vehicle images with different conditions, including low/high lighting, dusk, dirt, fog, and distorted images.

III. PROPOSED METHODOLOGIES

The structural diagram of the proposed LPD methodology is illustrated in Fig.3. It consists of two stages: training and testing. The training stage employs SVM and ELM learning algorithms, separately. Both training and testing phases use the same pre-processing and extraction methods. At the pre-processing stage, the ECHE and CLAHE techniques are applied to enhance the problematic part of vehicles images, while keeping the quality of the normal images during the enhancement process. Through the feature extraction stage, this study carefully selects the effective descriptors, MHOG and LBP, which are suitable for difficult conditions such as under low/high contrast, dirt, dusk, fog, and distortion problems. Finally, the detection stage uses a SVM and an ELM classifier, separately, as trained models to detect the LP region from the tested input vehicle image. The output results are saved for the recognition stage to obtain a complete ANPR

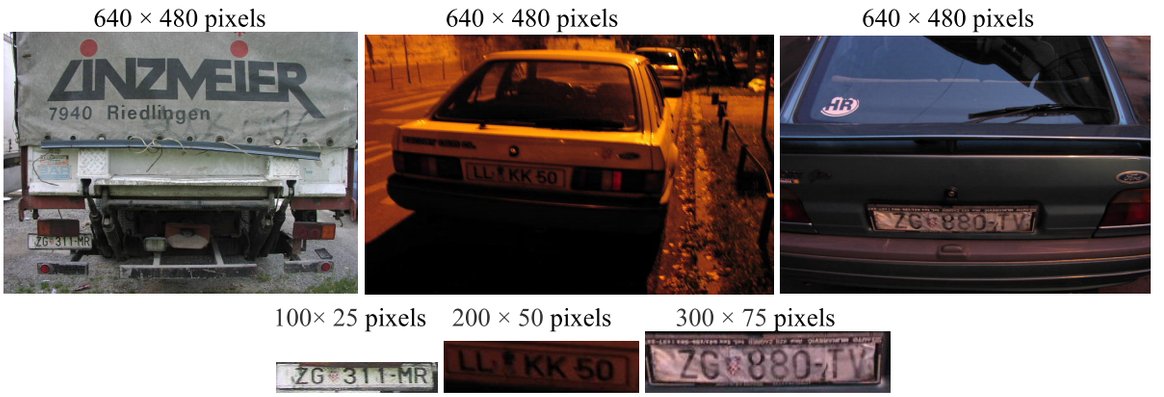

FIGURE 4. The different resolution for LP in the training dataset.

system. The details about the proposed method are presented in the next sections.

A. ENHANCEMENT STAGE FOR VEHICLE IMAGES

The proposed framework uses the texture and gray level features to detect the LP regions instead of color features which are very sensitive to the illumination and noise problems. The main purpose of this study is to detect the LP numbers under complicated conditions, for example under different illumination. Most previous studies converted the color images into grayscale ones for RGB reduction [26]. According to Saravanan [27] a color image IMRGB (i, j) has M × N dimensions. Where M is the height or the number of rows and N is the width or the number of columns in the image, and $0 \leq i \leq (M-1)$ and $0 \leq j \leq (N-1)$. IMRGB (i, j) was converted to a grayscale image, Gray (i, j), by Eq. (1) [27]:

$$Gray(i,j) = 0.2989 \times R(i,j) + 0.5870 \times G(i,j) + 0.1140 \times B(i,j) \quad (1)$$

where R(i, j), G(i, j), and B(i, j) are the three channels of colors, red, green and blue, respectively.

A large image resolution needs more time processing. In this study, an English car database has a consistent resolution of 640 × 480 pixels. In this study, a sliding window (M×N) will be used to scan an image from M×N resolution instead of scanning the whole image. The sliding window will be started to detect LP regions from M = 200 and N = 30. This process leads to reduce the processing time and obtain better detection results. As shown in Fig. 4, the LPs in the training dataset have three resolutions, 100 × 25, 200 × 50, and 300 × 75 pixels.

Referring to non-LP regions, there are various sources of noise along with the text in a vehicle image, such as surface textures, distortion, dusk, low/high lighting, and dirt. Those noises increase the bounding boxes during the detection stage.

In this study, we propose an enhancement pre-processing algorithm to reduce noise and improve the lighting conditions for complicated images without affecting on the quality of the images in normal conditions. The steps of the ECHE combined with the CLAHE algorithm are as follows:

1) Apply a Gaussian filter with the standard deviation $\sigma = 0.25$,
2) Apply the cumulative histogram equalization (CHE) method,

$$P_x(i) = P(x = i) = n_i/n, \quad 0 \leq i < L \quad (2)$$

where L is the total number of grayscale levels in an image which is typically 256 and n is the image pixels. $P_x(i)$ is the image's histogram of the pixel value i, which is normalized to [0, 1].

3) Calculate the histogram of the cumulative distribution function (CDF), which is also an image accumulated normalized histogram and defined as

$$CDF_x(i) = \sum_{j=0}^{i} P_x(j) \quad (3)$$

4) Calculate the new values of the histogram through the general histogram equalization formula,

$$CDF_y(i) = iC \quad (4)$$

where C is a constant in the range of [0-L], which is also needs a linearized CDF across the new value range y.

5) Apply the contrast-limited adaptive histogram equalization (CLAHE) method with the standard deviation $\sigma = 0.02$, and
6) Build a new enhanced image by replacing each gray value in the image with the new gray values.

The performance differences between the CHE, CLAHE, and the proposed pre-processing methods (ECHE+CLAHE) can be observed on Figs.5 (a), (b), and (c), respectively. From Figs. 5(a), (b), and (c), note that the proposed pre-processing method reduced the range of feature dimensions. Some results applied on testing vehicle images by the algorithm are shown in Fig. 6.

The grayscale image histogram has 256 bins by default. It represents the distribution function of image intensities. The *imhist* function in Matlab shows the histogram plot

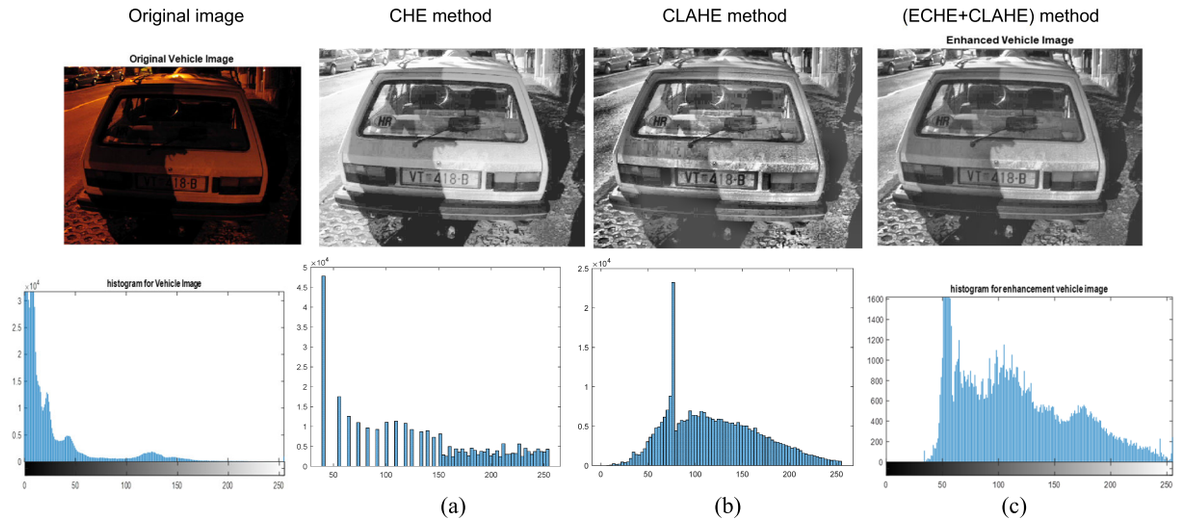

FIGURE 5. The output of unenhanced image (left) compared to three preprocessing enhancement (a), (b), (c) to the right, (a) is the CHE method, (b) is the CLAHE method, and (c) is the proposed preprocessing method (ECHE+CLAHE) (X axis = the range of features' values in each bin, Y axis = the number of features' values appearing in each bin range).

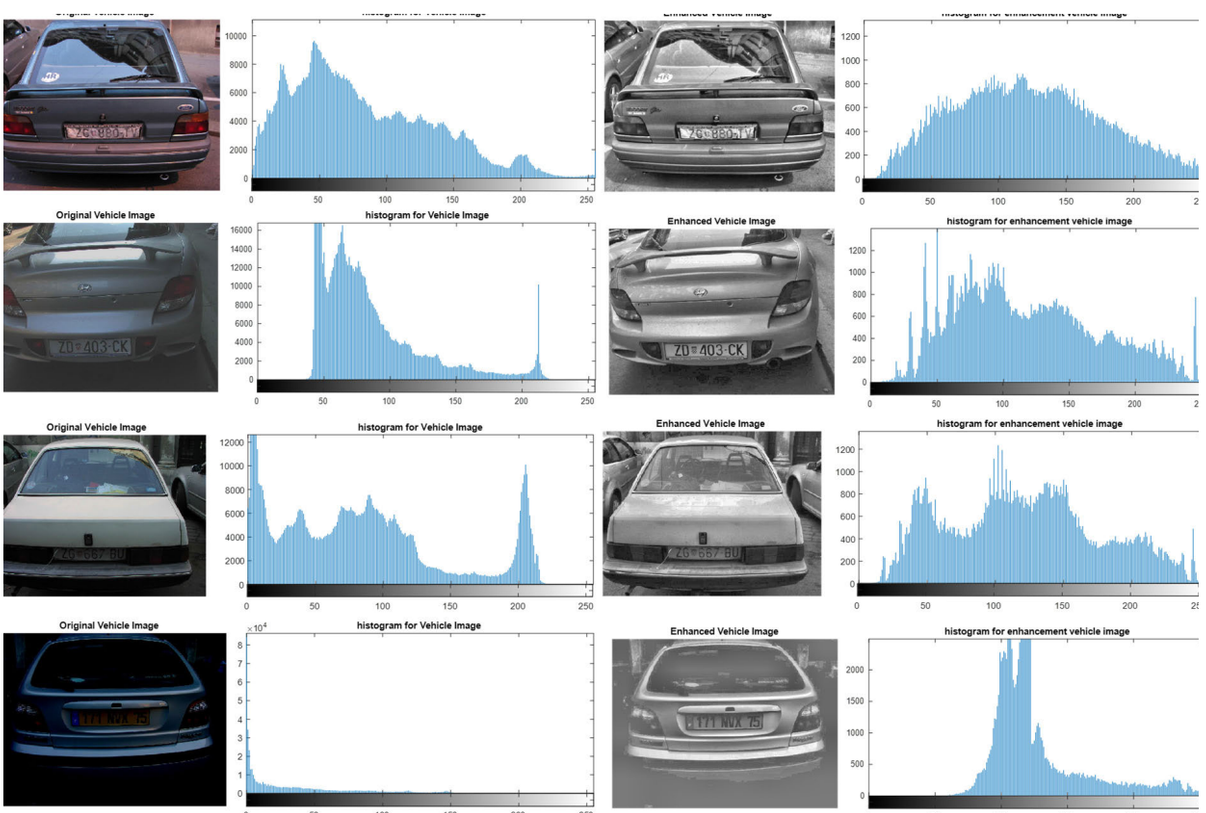

FIGURE 6. The output with the histogram for the testing complicated vehicle images in the dataset. The histogram displays how the enhancement algorithm works (X axis = the range of features values in each bin, Y axis = the number of feature values appeared in each bin range).

(X, Y), where X is the spaced bins, and each bin represents the range of feature values, Y is the number of pixels within each range. From the Fig. 6, we can observe the results by the enhancement method for different types of both, clear and complicated vehicle images. Using the histogram information helps decrease the value ranges of the unwanted features.

The next subsection presents more details about the strong descriptors used in this study.

B. THE HOG AND LBP DESCRIPTORS

This study uses two powerful descriptors, HOG and LBP, to extract key features from complicated LP images. They are used in this work for many reasons as described in this paper. The description about the extraction descriptors is given in this section.

1) THE HOG DESCRIPTOR

The HOG descriptor is one of the common imaging descriptors in the area of the computer vision [28]. It delivers good results in different computer vision applications, such as face detection [29], vehicle detection [30], and text extraction [31]. In addition, it is not sensitive to lighting changes and small offsets. It can effectively describe the edge features of an object. Therefore, it provides a rough estimation of the object appearance and shape. The steps for the extraction of the HOG features were as follows:

a. Used the median filter with HOG and assumed that the input to the MHOG descriptor is a window G from the enhancement LP grayscale image. The first step for MHOG is to divide G into non-overlapping blocks of 8×2 pixels. Each block is divided into small regions or called cells (8×8 pixels). The cells are combined into adjacent blocks of 2×2 cells, and we concatenate those four cells histogram into one block features. The horizontal and vertical gradients are obtained for each pixel inside the cell. The simplest technique to do that is by using the 1D Sobel operators ([-1, 0, 1] and [-1, 0, 1] T) [32]:

$$G_x(x, y) = G(x + 1,y) - G(x - 1,y) \quad (5)$$

$$G_y(x, y) = G(x,y + 1) - G(x,y - 1) \quad (6)$$

where G_x (x, y) is the horizontal gradient, and G_y (x, y) is the vertical gradient. x and y are the row and column indexes, respectively.

b. After that, the gradient is transformed into the polar coordinates of x and y directions with the angle set to between 0 and 180 degrees. The gradient magnitude μ and the direction of pixel θ are calculated according to Eqs. (7) and (8).

$$\mu(x, y) = \sqrt{G_x^2 + G_y^2} \quad (7)$$

$$\theta(x, y) = \frac{180}{\pi}(tan_2^{-1}\left(G_x, G_y\right) mod\pi) \quad (8)$$

where tan_2^{-1} is the inverse tangent for the quadrant, which produces values between $-\pi$ and π.

c. The MHOG histogram in each cell is computed, and all the values are joined into 9 bins, meaning the cell is divided into nine gradient directions from 0° to 180° orientations. In this way, we can gain different gradient orientations due to different contrasts among images. Therefore, the block gradient histogram should be normalized. The block normalization technique is a mid-solution for changes in illumination conditions. The cell histograms need to be normalized to reduce the contrast changes between the images for the same object. The normalization process can be done on the histogram vector by using L1-norm or L2-norm. The L1-norm provides lower reliability than L2-norm [28]. This study uses the L1-norm for the normalization of the MHOG features vector.

d. Finally, we collect the MHOG for all overlapping blocks features in the detection window, and combine them into a final MHOG features vector for classification. The steps of generating the MHOG descriptor from an LP image are shown in Fig. 7. The extracted features' histograms are used as the input to the SVM and ELM classifiers, separately, to build the final LP detector.

2) THE LBP DESCRIPTOR

The second powerful descriptor used in this study is the LBP. It is employed to extract different features for several reasons [24]. The LBP is effective for different illumination conditions and can solve the scale invariance and occlusion problems. The first LBP descriptor was presented by Ojala *et al.* [24]. The study divided the trained image into cells and labelled the pixels in each cell using a 3×3 window, then selected the center pixel value of the cell as a threshold. The center pixel value was then compared with the gray values from neighboring 8 pixel cells. If it was smaller than the neighbouring pixel value, the location of the pixel was marked by 1, otherwise 0. Therefore, the 8 neighboring values in the 3×3 window could produce 8 binary numbers. The 8 binary numbers are usually converted to the decimal numbers which are the LBP code. In total there were 256 grayscale values. The LBP values of the window for the central pixel are utilized to reflect the texture information in the region (see Fig. 8). The LBP code value of the center pixel is calculated by Eq. (9):

$$LBP\,(x_c, y_c) = \sum_{n=0}^{i-1} f(p_n - p_c)2^n \quad (9)$$

where p_c is the brightness value of the center pixel value (x_c, y_c), p_n is the brightness value of the n point in the i neighbouring domain. $f(x)$ function is defined as:

$$f\,(x) = \left\{ \begin{array}{ll} 1, & x \geq 0 \\ 0, & x < 0 \end{array} \right\} \quad (10)$$

For example, the pattern of 11001111 includes more than two transitions. Therefore, it is called uniform patterns. The single LBP descriptor can produce much fewer uniform patterns without loss of useful features. After the LBP operator labelled image, $f_l\,(x, y)$ has been obtained. The histogram of the LBP can be defined as:

$$H_i = \sum_{x,y} I\left\{f_l\,(x, y) = i\right\}, \quad i = 0, \ldots, n - 1, \quad (11)$$

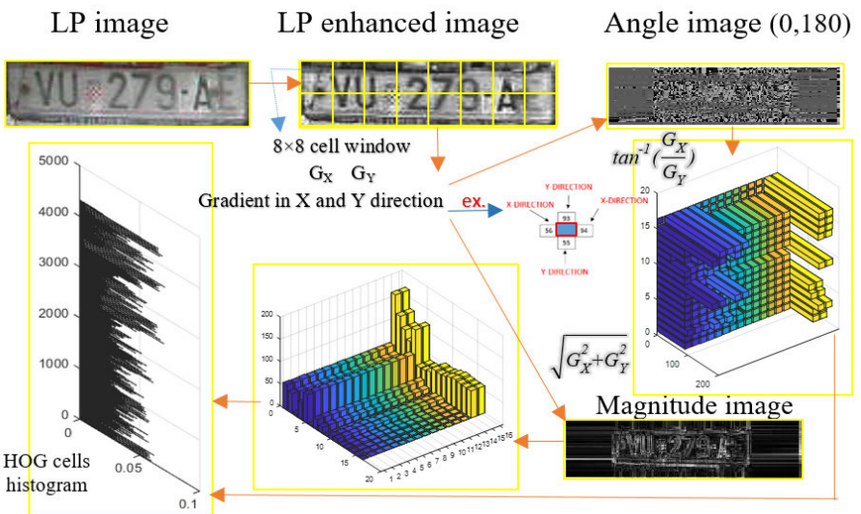

FIGURE 7. Steps of generating the MHOG descriptor for a LP image patch.

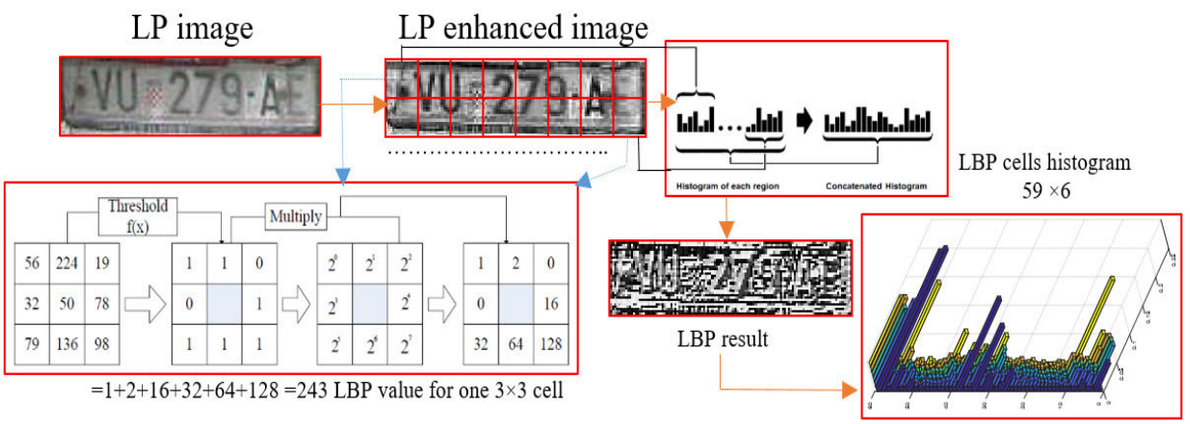

FIGURE 8. Steps of generating the LBP descriptor for LP images.

in which n is the number of labels that are produced by the LBP descriptor, and $I\{f(x)\}$ is 1 if $f(x)$ is true and 0 if $f(x)$ is false.

The features from each LBP region are concatenated into a maximum pooling features histogram vector. The steps for generating the LBP descriptor from an LP image are shown in Fig. 8. Finally, the extracted features histograms are used as the input to the SVM or ELM classifier to build the final trained LP detector. The LBPs are useful to remove the unwanted regions or noise from images [33].

C. FEATURE SELECTION USING SVM AND ELM CLASSIFIERS

Despite most of the learning algorithms being able to do the same job, their performance is heavily dependent on the pre-processing and extraction methods used. In this research, a deep learning classifier, such as a CNN, was also used. But it did not yield good classification results, especially with the HOG descriptor. A CNN classifier normally requires a fixed-resolution for input images [34], while there are three resolutions included in our training dataset. Thus it is not easy to conclude which learning algorithm is better than others. In this study, two popular classifiers were used, SVM and ELM, to evaluate the performance of the proposed method. All the extracted features using the MHOG and LBP procedures are fed to the classifiers separately, and build an ensemble of strong LP detectors to detect different LP features. To make the trained model computationally efficient in terms of the processing time and accuracy, most discriminative features should be extracted, and redundant information and noise are removed. This paper applies a SVM or ELM classifier to train and classify the extracted features. The descriptions of the classifiers are given in this section.

1) SUPPORT VECTOR MACHINE (SVM)

The SVM is one of the supervised machine learning algorithms, that is commonly used for classification and regression [17]. It can be seen as a type of artificial intelligence

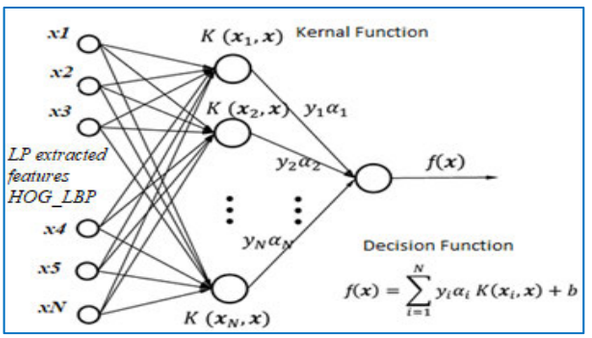

FIGURE 9. The workflow of the support vector machine network.

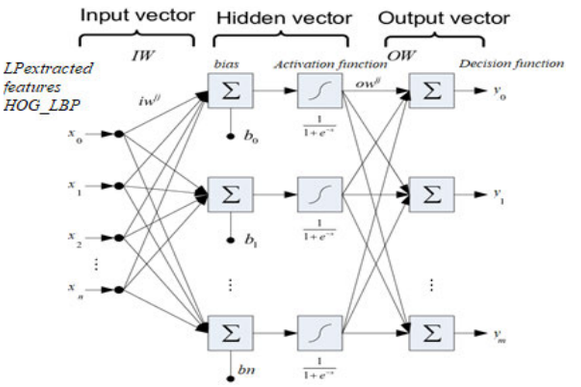

FIGURE 10. Extreme learning machine workflow.

network, called a support vector network [18]. The main objectives of a binary SVM is to separate the margins in the feature space of the two different classes α_i, positive and negative (see Fig. 9).

In general, linear functions are utilized as a separating hyperplane in the feature space x_N. It is used in pattern recognition and object detection for the generalized linear classifier. Then, it gives a decision surface maximized by employing an optimization approach. A kernel function K (x_N, x), such as linear, nonlinear, gaussian kernel, sigmoid, polynomial, radial basis function etc., is used to achieve better classification performance. When using a kernel function K, the scalar output $y_N\alpha_N$, can be implicitly calculated in the kernel feature space N with a threshold bias value b. Refer to the references in [17] for more details about the SVM classifier.

2) EXTREME LEARNING MACHINE (ELM)

Although the neural network and support vector machine are widely used [35], [36], those types of algorithms have a low learning speed for a reasonable classification accuracy [37]. The ELM is a single hidden-layer feedforward neural network (SLFN), initially proposed by Huang et al [38]. It can be viewed as a variant of a random vector functional-link (RVFL) network classifier [39] without direct links and bias terms. It ignores the need for tuning parameters in the training phase and hence minimizes the training time compared to the traditional neural networks. The ELM workflow is illustrated in Fig. 10, where the network input *(IW)* vector obtained from the input extracted features of the HOG and LBP multiplied by the input weight *IW* matrix. The *IW* and the hidden-layer bias *b* values are randomly assigned, while the output weights *OW* are analytically calculated. After that, the results are added to the bias vector *b* to create the input to the *"sigmoid"* activation function and produce a good output layer. The *b* value as the threshold helps the input layer to decide the activation of neurons and increases the flexibility of the training model. Without bias, the neurons do not pass to the other network layers. Finally, the output of the *"sigmoid"* function is multiplied with the network output weight *OW* matrix to produce the final results *ym* or decision function. Refer to reference [40] for more details about the ELM classifier.

D. THE OVERLAPPING AND REDUNDANT BOUNDING BOXES

In this study, a sliding window is applied to scan vehicle images. The MHOG and LBP features are extracted at each stage of the sliding window. After that, the trained classifiers, SVM or ELM, are applied to detect the LPs. If the classifier detects the LP, the bounding box records the region of interest. When the scan process is completed on the whole testing image, many bounding boxes are detected around the LP region in the vehicle image. Therefore, a suppression technique is applied in order to remove the overlapping and redundant bounding boxes from the detection area. Fig. 11 shows an example of the overlapping bounding boxes problem with both classifiers, SVM and ELM.

As shown in Figs. 11 (a) and (b), the vehicle image has six and 15 overlapping bounding boxes with SVM and ELM, respectively. This is an open problem, no matter which detection method is used, whenever the LP area was correctly detected. Here all those redundant boxes refer to the same LP, a technique to suppress the smaller bounding boxes and keep the larger bounding boxes is required, as shown in Figs. 12 (a) and (b).

There are many ways to solve the overlapping bounding boxes problem. A position-based method, or mean-shift, is a generalized as the way to detect an object by searching the candidate objects which have the highest similarity with the detected one [41]. In this study, the proposed method applies the mean-shift algorithm to reduce the similar candidate objects or overlapping bounding boxes for LPs. It is used to capture multiple regions in the space of the bounding boxes by utilizing the coordinates of the redundant boxes, *(x, y),* as well as the current scale of the tested image (logarithm). A mean-shift tracking technique is used to track the detected LP in a vehicle image. The process of the mean-shift method is shown in Fig. 13.

This method starts with searching around the overlapping windows of the LP region. The windows have the same x coordinate as the LP frame. Then, the average of y coordinates which have different positions to the start point x is calculated and removed. The results from using this algorithm are

FIGURE 11. (a) The output of the proposed method using the SVM without the mean-shift algorithm; (b) The output of the proposed method using the ELM without the mean-shift algorithm.

FIGURE 12. (a) The output of the proposed method using the SVM with mean-shift algorithm, (b) The output of the proposed method using the ELM with mean-shift algorithm.

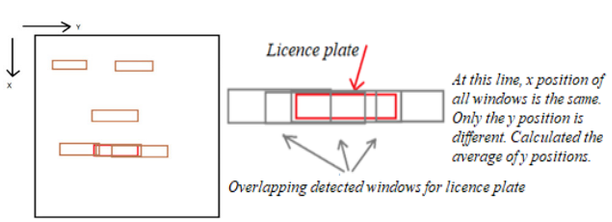

FIGURE 13. Steps of the mean-shift algorithm.

very satisfactory, with low false positive values and higher accuracy rates. Also, this algorithm relies on the effective classifier of the SVM or ELM that is selected to produce good results. Refer to reference [41] for more details about the mean-shift algorithm.

IV. DATABASE

The proposed method is tested on two groups of databases: 1) An English car database including 510 vehicle images under different conditions [42]. 2) An extended English car database by Al-Shemarry *et al.* [25] covering 1540 vehicle images under complicated conditions, such as too dark, blurry, distortion, and low/high contrast environments (see Fig. 14). The second database is an extension of the first English car database as Al-Shemarry *et al.* [25] changed the lighting, blurry, distortion conditions using online photo editor application to make it more challenging [43]. From the two databases, 530 vehicle images were randomly selected for the testing and 1520 were used for the training LPs dataset. The total number of vehicle images is 2050. In addition, this method is also applied to different vehicle images with Arabic or Chinese language on the licence plates. The vehicle images are downloaded from the Internet and resized into 480×640 resolution and are used to evaluate the performance of the LPD system as shown in Fig. 15.

The extended database also includes the rotated images with different LP angles, such as 45°, 30°, 20°, 15°, and 5°. Moreover, the training dataset contains various illumination conditions with three LPs resolutions of 100×25, 200×50,

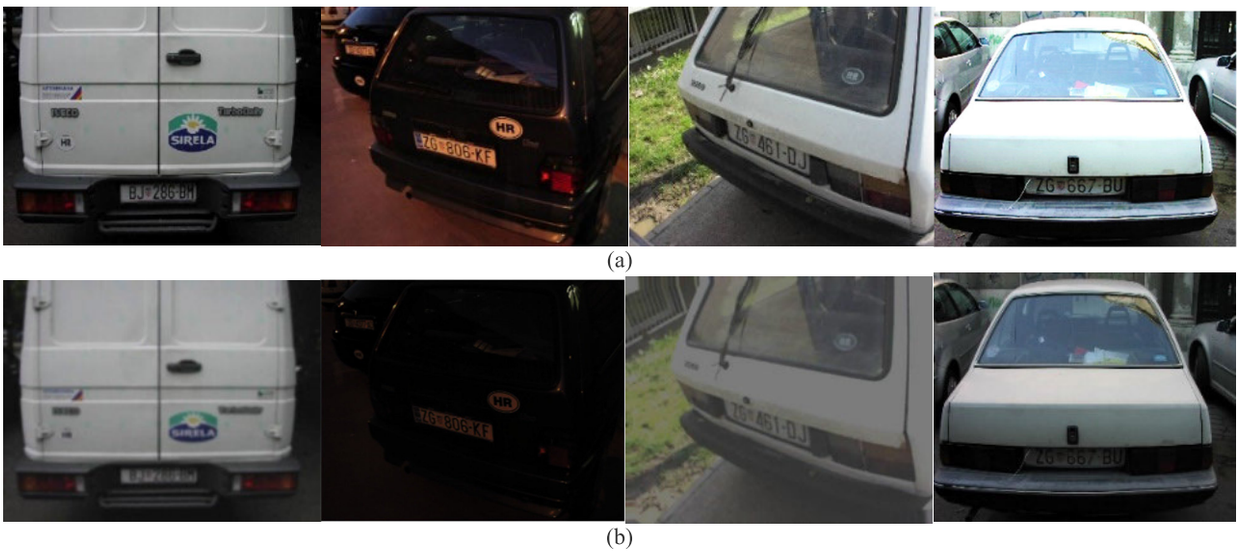

FIGURE 14. (a) Examples of vehicles images in the original English vehicles database with simple conditions; (b) Examples from the extended English vehicles database after photo editing.

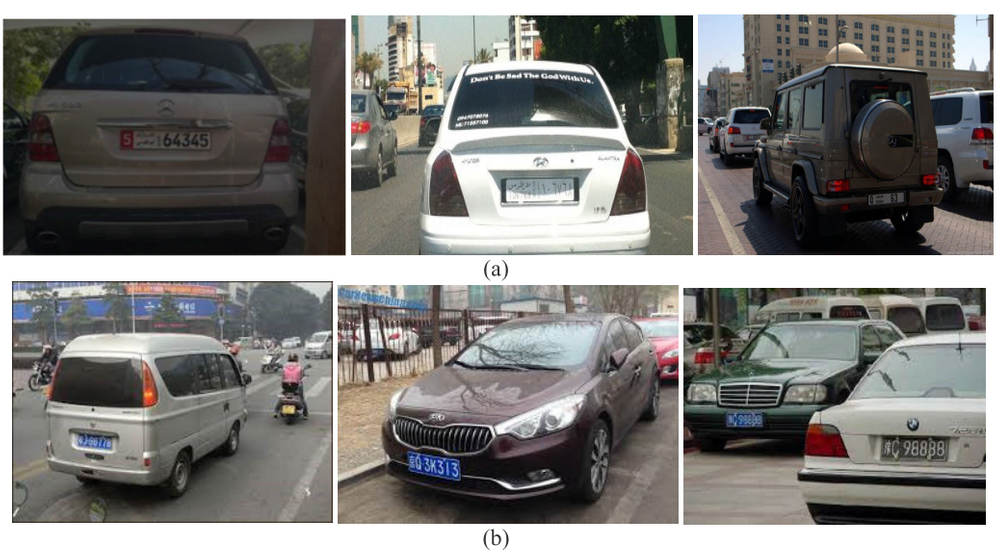

FIGURE 15. (a) Examples of Arabic vehicles images; (b) Examples of Chinese vehicles images.

and 300 × 75 to enable the LPD system to capture LPs from complicated or low-quality images. Fig. 16 shows some of the training LPs images under difficult and simple conditions. The experimental results showed that all the key characteristics have been captured from the 1520 training images.

V. EXPERIMENTS AND RESULTS

All the experiments by the proposed method are implemented on a computer with 3.4 GHz Intel Core i7-4770, 16GB of RAM using MATLAB, version R2017b. In this section, the descriptions of MHOG and LBP features analysis and features selection processes by SVM and ELM classifiers are firstly presented. Secondly, the performance evaluation of the proposed method is evaluated using the detection and object localization metrics. Thirdly, the performance comparison using the receive operating characteristic (ROC) curve between the SVM_MHOG_LBP and ELM_MHOG_LBP is provided. Finally, the detection accuracy and time efficiency of the proposed method are compared with the newest detection methods that also used the same database [25], [44], [45] as the one used in this study.

A. FEATURE ANALYSIS AND SELECTION

Feature analysis is a very important step for any classification problems. This study combines the MHOG and LBP features into a features vector. The SVM and ELM classifiers are

FIGURE 16. Examples of LPs training images under simple and complicated conditions.

TABLE 1. The dimension of training models using SVM and ELM classifiers.

Method	TM1 (100×25)	TM2 (200×50)	TM3 (300×75)	Average TA
SVM_MHOG_LBP	features	features	features	99.786%
Class 1	62	110	71	
Class 2	64	111	71	
Class 3	61	105	66	
Class 4	62	112	72	
Class 5	64	109	68	
Total features	313	547	348	
ELM_MHOG_LBP	*640*	851	1202	100%

TM: Trained Model; TA: Training Accuracy

TABLE 2. The detection results for the proposed method using the SVM and ELM classifiers.

Method	No. of Testing Images = 530, TN= 50 Images					
	FP	TP	FN	TN	DR	AR
SVM_LBP	15	483	47	40	91.13%	89.40%
SVM_MHOG	25	478	52	44	91.57%	87.14%
SVM_MHOG_LBP	**9**	**528**	**2**	**48**	**99.62%**	**98.12%**
ELM_LBP	14	480	50	42	90.56%	89.07%
ELM_MHOG	21	473	57	39	89.24%	86.77%
ELM_MHOG_LBP	**13**	**515**	**15**	**43**	**97.16%**	**95.22%**

AR: Accuracy Rate

used separately, to detect LPs from vehicle images. With the MHOG features, each bin includes the feature magnitude for 8 × 8 cells for a specific direction. High feature values indicate the most discriminative bin. The complete MHOG operator contains the magnitude values in all 180 directions. Therefore, it is a high value around the 20, 60, 100, 140, and 180 degrees. For the LBP descriptor each bin contains features values for 3 × 3 cells. The extracted features for the three LP resolutions of 100 × 25, 200 × 50, and 300 × 75 using the MHOG and LBP descriptors are shown in Fig. 17.

The dimensions of the extracted feature values for the three resolutions above are 1517, 1784, and 1582, respectively. The linear SVM and the kernel ELM classifiers were applied to select strong subset feature values. The information about features selection for both classifiers are displayed in Table 1.

In this study, the linear kernel function for the SVM was used for learning the classes of LPs and non-LPs. The SVM classifier was tested with 5-fold cross validation for three dimensions features values as well as three LPs resolutions of 313, 547, and 348, respectively. From Table 1 the training dataset includes three detectors or training models with different dimension features values. Each SVM trained model with 5-fold cross validation contains five ensemble classes for LPs features. The weighting values for three SVM training models are 6.591, 5.605, and 6.321, respectively, with different bias values. The bias is a special parameter in the SVM. The classifier without this value would always go to the origin. Also, the SVM does not give the separating hyperplane for the maximum features margin without the bias term. The ELM was tested with 550 input hidden neurons, and the input neurons for the three LP resolutions are 640, 851, and 1202, respectively. The ELM classifier produced three training models for the three LP resolutions with a training accuracy rate of 100%.

B. PERFORMANCE EVALUATION

The proposed method is evaluated using detection and object localization metrics.

1) DETECTION METRICS FOR LPD

Several assessment measures are used to check the performance of the proposed detection system. The assessment metrics include the number of objects that are correctly detected, falsely detected, or miss-undetected by the system [46]. Also, the detection based metrics are used to evaluate the system under test (SUT) performance. For those metrics, all the objects are validated to see if there is a matching between SUT and the ground truth (GT). The detection metrics used in this study to evaluate the LPD system are as follows:

- FP (false positive): means that the LP is detected by the SUT, but it is not in the GT.
- FN (false negative): indicates that the LP exists in the GT, but it is not detected by the SUT.
- TP (true positive or correct detection): means that the LP exists in both the GT and the SUT.
- TN (true negative): indicates that the LP does not exist in the GT and by the SUT.

We added in the car English car database 50 vehicle images without the LP that means the TN which refers to the vehicle image without the LP object inside it. This is a very important step to validate the detection system performance.

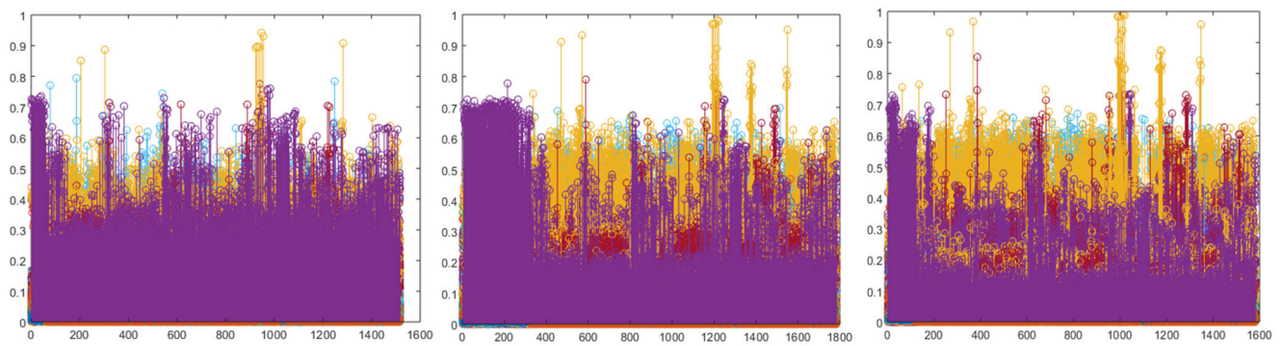

FIGURE 17. (a) The output of the extracted MHOG_LBP features for an LP with 100 × 25 resolution; (b) The output of the extracted MHOG_LBP features for an LP with 200 × 50 resolution; (c) The output of the extracted MHOG_LBP features for an LP with 300 × 75 resolution (For histogram: X axis = the range of features values in each bin, Y axis = the features values appearance in each bin range).

The detection and accuracy rates can be calculated as follows:

$$Detectionrate(DR) = TP/(TP+FN) \tag{12}$$

$$Accuracy = (TP + TN)/(TP + TN + FP + FN) \tag{13}$$

The *DR* is the proportion of the true positive result that is truly predicted as a positive result by the detector, while the accuracy rate is the proportion of the true results for both positive and negative LP objects in the *GT*. The detection results are shown in Table 2.

From Table 2, it is noticeable that the combination of the extracted features from both the MHOG and LBP improves the detection results. The SVM_MHOG_LBP method outperforms other methods in terms of the detection accuracy rates. Some examples of the detection results for the proposed method are shown in Fig.18.

It was observed that all LPs were detected with very low FPs values, and fewer redundant bounding boxes appeared under difficult conditions. Also, some FPs were noticed when some objects in the vehicle image looked like an LP (for example, commercial signs and the vehicle logos).

2) OBJECT LOCALIZATION METRICS

The recall (RR) or detection rate (DR), precision (PR), and F-measure (F-m) rates [47] at a matching confidence of $\delta \geq 0.5$ are used to evaluate the LP localization performance. Those metrics are defined as follows:

$$RR = TP/(TP + FN) \quad when\ \delta \geq 0.5 \tag{14}$$

$$PR = TP/(TP + FP) \quad when\ \delta \geq 0.5 \tag{15}$$

$$F - m = 2(PR \times RR)/(PR + RR) \tag{16}$$

PR is the proportion of the actual negative objects that the detection system predicted correctly as negatives [47]. The matching confidence assumption δ is defined as follows:

$$\delta = \{Bb \cap GT/Bb \cup GT, GT \subseteq Bb\} \tag{17}$$

where *Bb* denotes the predicted area of the LP bounding box. The detection performance is analyzed with the confidence $\delta \geq 0.5$. It means that *Bb* encloses to the related *GT* while the area of the former is twice of the latter. If δ is too big, the predicted *Bb* would be much larger than the *GT*, which does not make any sense to the LP detection ratio. The confidence value determines directly from the strong classifier. Table 3 shows the object localization metrics of the proposed method.

TABLE 3. The performance results by the proposed LPD system.

Method	RR	PR	F-m
SVM_LBP	91.13%	96.98%	93.96%
SVM_MHOG	91.57%	95.02%	93.26%
SVM_MHOG_LBP	**99.62%**	**98.32%**	**98.96%**
ELM_LBP	90.56%	97.16%	93.74%
ELM_MHOG	89.24%	95.74%	92.66%
ELM_MHOG_LBP	**97.16%**	**97.53%**	**97.34%**

We can observe from Table 3 that the results of object localization metrics for *SVM_MHOG_LBP* are better than other methods' results.

C. THE RECEIVE OPERATING CHARACTERISTIC (ROC) CURVE

This study uses a combined features vector extracted by the HOG and LBP, and employs a SVM or an ELM classifier to detect the LPs from complicated vehicle images. The efficiency of the proposed method is evaluated using the receiver operating characteristic (ROC) curve. The ROC curve is a useful tool for organizing the work of the classifiers and displaying their quality of the performance [48]. It is known as a performance metric for comparing and evaluating algorithms [48], [49]. The ROC curve depends on four parameters, true positive rate (*TPR*) or *RR* rate (see Eq. 9), false positive rate (FPR), positive predictive value *(PPV)* or

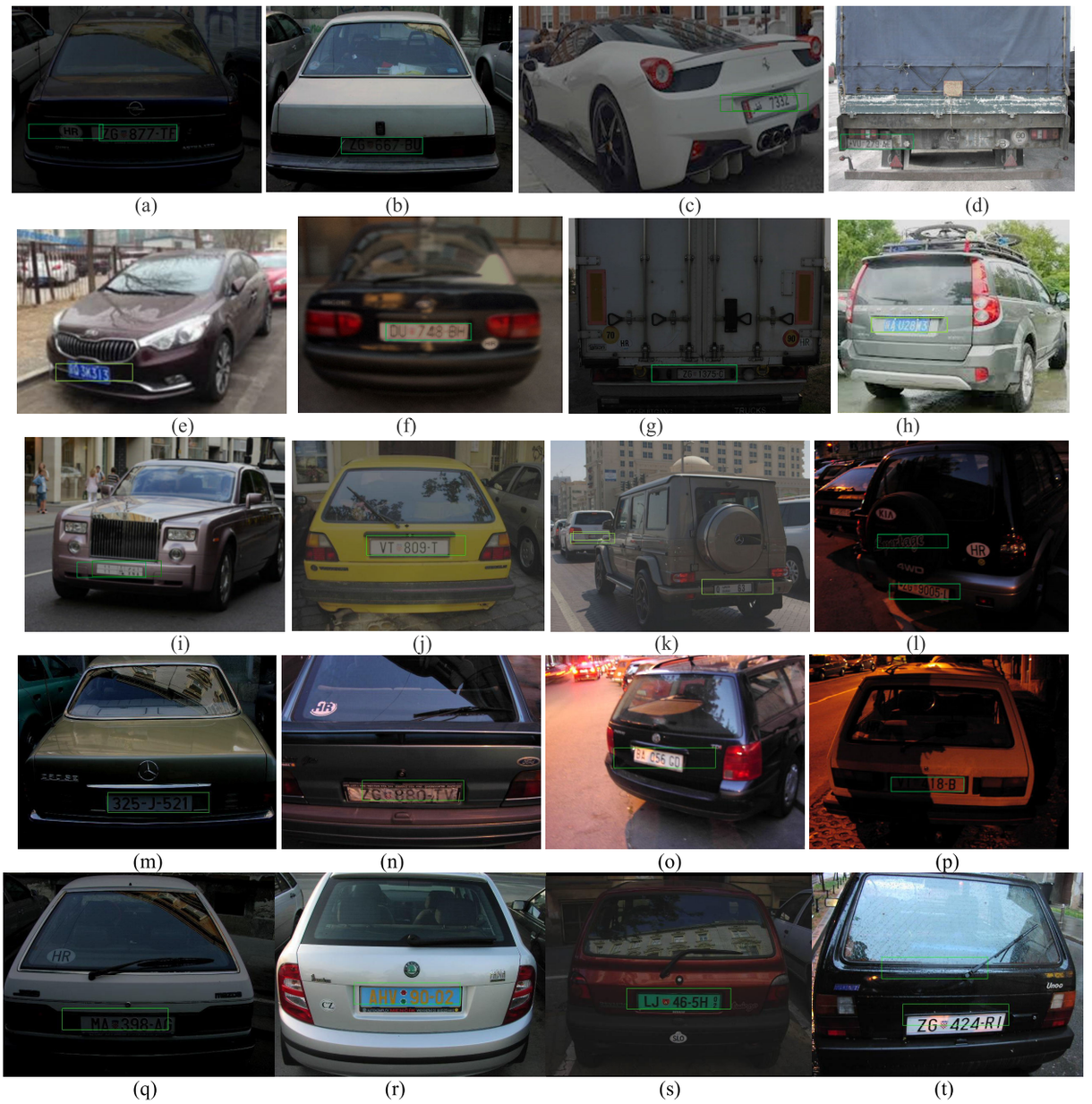

FIGURE 18. Examples of the successful detection results by the proposed method for complicated cars images with low light and dirt (a), (b), (d), (e), (q); with various views points (c), (h), (i), (k), (l), (o); with dusk and fog (a), (e), (f), (i), (m); with distortion (d), (e), (k), (p), (n), with different color (h), (r), (s), (t), and with low/high contrast (f), (l), (m), (o), (p), (r) problems.

PR rate (see Eq. (15)), and negative predictive value *(NPV)*. Those parameters are defined as follows:

$$FPR = FP/(FP + TP) \tag{18}$$

$$NPV = TN/(TN + FN) \tag{19}$$

The ROC results from the SVM and ELM classifiers are reported in Figs. 19, 20, and Table 4.

The ROC curve for the SVM with MHOG_LBP features is better than that for the ELM with MHOG_LBP. The TPR and FPR from the SVM_MHOG_LBP are improved by 2.46% and 0.787%, respectively, in comparison to those by the ELM_MHOG_LBP. The area under curve (AUC) values are between 0 and 1.

The high value of the AUC is a better measure for evaluating the performance of the proposed method than the accuracy rate [49]. The AUC for the SVM_MHOG_LBP is better than the ELM_MHOG_LBP of 99.99% and 99.20%, respectively.

D. RUN TIME

The runtime is a key indicator of a system performance. Table 5 shows the average running time per vehicle image

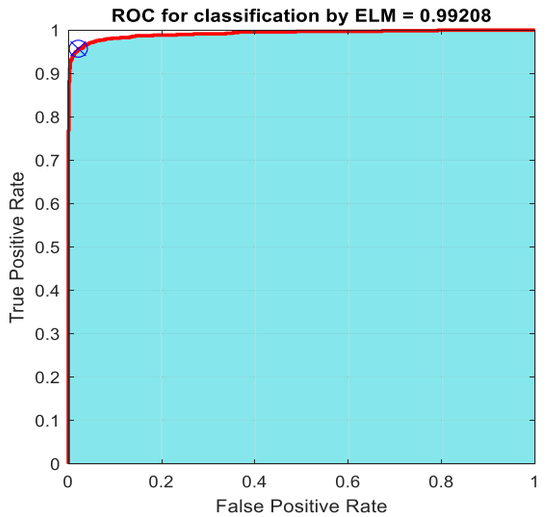

FIGURE 19. The ROC curve for the MHOG_LBP features classification using the ELM.

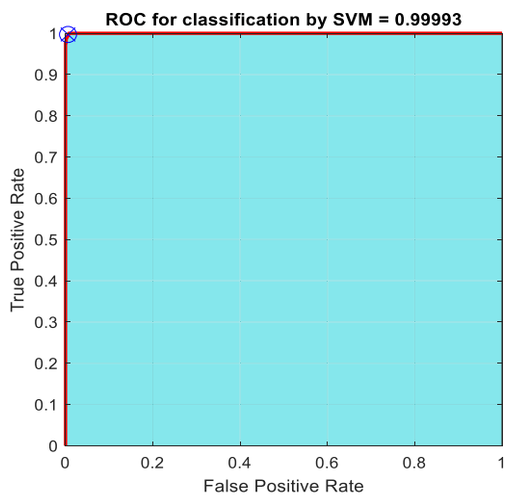

FIGURE 20. The ROC curve for the MHOG_LBP features classification using the SVM.

for the total and the three stages of preprocessing, extraction and detection by the proposed LPD system. The implementation time for the SVM_MHOG_LBP was much shorter than that for the ELM_MHOG_LBP method under both ordinary and complicated conditions. The proposed method makes the LPD system reliable for real-time applications through removing the unwanted bounding boxes and decreasing the running time.

VI. COMPARISON WITH EXISTING METHODS

In this section, the proposed method is compared with the state-of-the-art license plate detection methods that used the same database of English car plates [25], [44], [45], [50]. The performances are compared using the measures of the *RR* and *PR* rates as well as the F-m rate. Azam and Gavrilova [45] reported a genetic algorithm depending on the HOG features with a mixture of binary classifiers to classify LP and non-LP images. To improve the classification performance, the genetic algorithm was applied to select the best features subset. The method used a mixture of binary classifiers of k-nearest neighbor, SVM, decision tree, and linear discriminant analysis. It achieved some good results under different conditions, but it required a high-contrast preprocessing method to improve images. This leads to increase the false positive rate. Raghunandan, *et al.* [44] proposed a mathematical model using a Riesz fractional operator to enhance the details of LP edges' information. That method worked well as long as there was a clear LP shape in the image. It was not robust for distorted images and it was time-consuming with a low *RR* rate. Yousif, *et al.* [50] presented a novel methods based on genetic algorithm (GA) to identify LPs under limited conditions. Henry, *et al.* [51] designed a deep ALPR system to identify multinational LPs. Their proposed system included three steps: LP detection, LP recognition, and multinational layout LP detection. It achieved good results under good conditions but it was not robust or perform satisfactorily for complicated vehicle images. Also, Al-Shemarry, *et al.* [25] produced a new and efficient descriptor, with multi-level extended local binary patterns (MLELBP) to extract difficult features' using three neighbouring feature dimensions under complicated conditions. The input image was resized to make the proposed method work without any limitations related to standard vehicle image resolution and save the processing time. The ELM was used to build the trained model and obtain good detection results. In this method, the multi-levels preprocessing in the extraction stage leads to getting high feature dimensions which causes increases in the false positive rate. In addition, the resizing image process is not always successful especially with distorted images that could lead to loss of

TABLE 4. The performance results from SVM and ELM classifiers with the MHOG_LBP features, using ROC curve parameters.

Method	SVM_HOG_LBP	ELM_HOG_LBP
AUC	99.99%	99.20%
FPR	1.67%	2.46%
TPR	99.62%	97.16%
PPV	98.32%	97.53%
NPV	96%	74.17%
CA	99.78%	96.92%

CA: Classification Accuracy

TABLE 5. The average run time for the proposed method for each stage in the SVM_MHOG_LBP and ELM_MHOG_LBP schemes.

Stages	Proposed method	
	SVM_MHOG_LBP	ELM_MHOG_LBP
Pre-processing	0.0519*ms*	0.0519*ms*
Extraction	1.7260*ms*	1.7260*ms*
Detection	0.4408*ms*	1.0089*ms*
Total test time	2.2187*ms*	2.7868*ms*
Training Time	201.835*ms*	116.087*ms*

TABLE 6. Comparisons of the proposed method with the existing state-of-the-art methods in terms of the *RR, PR,* and *F-m* rates.

Method	*RR*	*PR*	*F-m*
Azam and Gavrilova [45]	91.3%	NR	NR
Raghunandan et al. [44]	79.4%	84.6%	81.9%
Al-Shemarry et al. [25]	99.10%	98.2%	98.65%
Yousif, et al. [50]	85.43%	97.86%	91.22%
Henry, et al. [51]	99.76%	98.85%	99.30%
Proposed SVM_MHOG_LBP	**99.62%**	**98.32%**	**98.96%**

NR: Not Reported

important feature values. Therefore this study proposed a new enhancement preprocessing method and used the mean-shift technique with a detector to reduce false positive values and decrease the processing time. The performance results of the proposed detection method and latest detection methods are reported in Table 6. Note from Table 6 that the proposed method achieved the best detection results compared with the existing methods in terms of *RR*, *PR*, and *F-m* rates.

VII. CONCLUSION AND FUTURE WORK

This study proposed a new preprocessing method to improve the LPD system performance for complicated vehicle images by a Gaussian filter and the ECHE with the CLAHE algorithm. The MHOG and LBP descriptors were used to extract the representative LP features. The English car plates' database, Al-Shemarry *et al.* database, Arabic and Chinese vehicles images databases were used to evaluate the system performance under more difficult and complicated image conditions. The SVM and ELM classifiers were used to classify the extracted features, separately, for comparison purposes. An ensemble of strong detectors or trained models for three types of LP resolutions, 100×25, 200×50 and 300×75, were developed. From the experimental results, the SVM with the combined MHOG and LBP descriptors outperformed the ELM and the other methods with a single descriptor in terms of the detection accuracy rate. The proposed method was tested using different databases with simple and complicated conditions, such as fogy, low/high contrast, distorted and rotated LPs. It yielded excellent results. The detection and accuracy rates are 99.62% and 98.12%, respectively. The overall performance evaluation for the object localization metrics of the recall, precision, and F-measure rates are 99.62%, 98.32%, and 98.96%, respectively, with an FPR of 1.675%. Also, the ROC curve was used to compare and evaluate the results of the proposed method. The classification results of the ROC curve were very good for the SVM and ELM methods at 99.78% and 96.92%, respectively. The proposed method was also compared with the existing LP detection methods that used the same English car database. It showed that the proposed method performed better than those by other methods in terms of the efficiency and detection rate. The average runtime for the detection stage per vehicle image was 0.2408ms. The experimental results demonstrated that the proposed technique could be applied efficiently for real-time applications. We plan, in future work, to enhance the proposed detection method through using high-quality hardware and software components for reducing the overall detection time of the LPD system, that currently is 2.2187ms in total.

REFERENCES

[1] Z. Huang, Y. Yu, J. Gu, and H. Liu, "An efficient method for traffic sign recognition based on extreme learning machine," *IEEE Trans. Cybern.*, vol. 47, no. 4, pp. 920–933, Apr. 2017.

[2] D. Selmanaj, M. Corno, and S. M. Savaresi, "Hazard detection for motorcycles via accelerometers: A self-organizing map approach," *IEEE Trans. Cybern.*, vol. 47, no. 11, pp. 3609–3620, Nov. 2017.

[3] P. Pramkeaw, M. Ketcham, W. Limpornchitwilai, and N. Chumuang, "Analysis of detecting and interpreting warning signs for distance of cars using analyzing the license plate," in *Proc. 14th Int. Joint Symp. Artif. Intell. Natural Lang. Process. (iSAI-NLP)*, Oct. 2019, pp. 1–8.

[4] P. Gao, R. Yuan, F. Wang, L. Xiao, H. Fujita, and Y. Zhang, "Siamese attentional keypoint network for high performance visual tracking," *Knowl.-Based Syst.*, vol. 193, Apr. 2020, Art. no. 105448.

[5] P. Gao, Q. Zhang, F. Wang, L. Xiao, H. Fujita, and Y. Zhang, "Learning reinforced attentional representation for end-to-end visual tracking," *Inf. Sci.*, vol. 517, pp. 52–67, May 2020.

[6] M. S. Al-Shemarry, Y. Li, and S. Abdulla, "Ensemble of AdaBoost cascades of 3L-LBPs classifiers for license plates detection with low quality images," *Expert Syst. Appl.*, vol. 92, pp. 216–235, Feb. 2018.

[7] H. Zhang, W. Jia, X. He, and Q. Wu, "Learning-based license plate detection using global and local features," in *Proc. 18th Int. Conf. Pattern Recognit. (ICPR)*, 2006, pp. 1102–1105.

[8] K. Zheng, Y. Zhao, J. Gu, and Q. Hu, "License plate detection using Haar-like features and histogram of oriented gradients," in *Proc. IEEE Int. Symp. Ind. Electron.*, May 2012, pp. 1502–1505.

[9] W. T. Ho, H. W. Lim, and Y. H. Tay, "Two-stage license plate detection using gentle AdaBoost and SIFT-SVM," in *Proc. 1st Asian Conf. Intell. Inf. Database Syst.*, Apr. 2009, pp. 109–114.

[10] S. Lew, C.-S. Yi, W.-J. Lee, B.-R. Lee, K.-W. Min, and H.-C. Kang, "Extraction of the license plate region using HoG and AdaBoost," *J. Digit. Contents Soc.*, vol. 10, no. 4, pp. 597–604, 2009.

[11] L. Liu, L. Zhao, Y. Long, G. Kuang, and P. Fieguth, "Extended local binary patterns for texture classification," *Image Vis. Comput.*, vol. 30, no. 2, pp. 86–99, Feb. 2012.

[12] L. Xie, T. Ahmad, L. Jin, Y. Liu, and S. Zhang, "A new CNN-based method for multi-directional car license plate detection," *IEEE Trans. Intell. Transp. Syst.*, vol. 19, no. 2, pp. 507–517, Feb. 2018.

[13] M. Molina-Moreno, I. González-Díaz, and F. Díaz-de-María, "Efficient scale-adaptive license plate detection system," *IEEE Trans. Intell. Transp. Syst.*, vol. 20, no. 6, pp. 2109–2121, Jun. 2019.

[14] W. Weihong and T. Jiaoyang, "Research on license plate recognition algorithms based on deep learning in complex environment," *IEEE Access*, vol. 8, pp. 91661–91675, 2020.

[15] C.-N.-E. Anagnostopoulos, I. E. Anagnostopoulos, I. D. Psoroulas, V. Loumos, and E. Kayafas, "License plate recognition from still images and video sequences: A survey," *IEEE Trans. Intell. Transp. Syst.*, vol. 9, no. 3, pp. 377–391, Sep. 2008.

[16] S. Azam and M. M. Islam, "Automatic license plate detection in hazardous condition," *J. Vis. Commun. Image Represent.*, vol. 36, pp. 172–186, Apr. 2016.

[17] S. R. Gunn, "Support vector machines for classification and regression," *ISIS Tech. Rep.*, vol. 14, no. 1, pp. 5–16, 1998.

[18] C. Cortes and V. Vapnik, "Support-vector networks," *Mach. Learn.*, vol. 20, no. 3, pp. 273–297, 1995.

[19] W. Kusakunniran, K. Ngamaschariyakul, C. Chantaraviwat, K. Janvittayanuchit, and K. Thongkanchorn, "A thai license plate localization using SVM," in *Proc. Int. Comput. Sci. Eng. Conf. (ICSEC)*, Jul. 2014, pp. 163–167.

[20] S. Zain Masood, G. Shu, A. Dehghan, and E. G. Ortiz, "License plate detection and recognition using deeply learned convolutional neural networks," 2017, *arXiv:1703.07330*. [Online]. Available: http://arxiv.org/abs/1703.07330

[21] Y. Liu, H. Huang, J. Cao, and T. Huang, "Convolutional neural networks-based intelligent recognition of Chinese license plates," *Soft Comput.*, vol. 22, no. 7, pp. 2403–2419, 2017.
[22] S. Ding, L. Guo, and Y. Hou, "Extreme learning machine with kernel model based on deep learning," *Neural Comput. Appl.*, vol. 28, no. 8, pp. 1975–1984, Aug. 2017.
[23] P. Felzenszwalb, D. McAllester, and D. Ramanan, "A discriminatively trained, multiscale, deformable part model," in *Proc. IEEE Conf. Comput. Vis. Pattern Recognit.*, Jun. 2008, pp. 1–8.
[24] T. Ojala, M. Pietikainen, and T. Maenpaa, "Multiresolution gray-scale and rotation invariant texture classification with local binary patterns," *IEEE Trans. Pattern Anal. Mach. Intell.*, vol. 24, no. 7, pp. 971–987, Jul. 2002.
[25] M. S. Al-Shemarry, Y. Li, and S. Abdulla, "An efficient texture descriptor for the detection of license plates from vehicle images in difficult conditions," *IEEE Trans. Intell. Transp. Syst.*, vol. 21, no. 2, pp. 553–564, Feb. 2020.
[26] A. A. Gooch, S. C. Olsen, J. Tumblin, and B. Gooch, "Color2Gray: Salience-preserving color removal," *ACM Trans. Graph.*, vol. 24, no. 3, pp. 634–639, 2005.
[27] C. Saravanan, "Color image to grayscale image conversion," in *Proc. 2nd Int. Conf. Comput. Eng. Appl.*, 2010, pp. 196–199.
[28] N. Dalal and B. Triggs, "Histograms of oriented gradients for human detection," in *Proc. IEEE Comput. Soc. Conf. Comput. Vis. Pattern Recognit. (CVPR)*, 2005, pp. 886–893.
[29] H. Tan, Z. Ma, and B. Yang, "Face recognition based on the fusion of global and local HOG features of face images," *IET Comput. Vis.*, vol. 8, no. 3, pp. 224–234, Jun. 2014.
[30] D. Sun and J. Watada, "Detecting pedestrians and vehicles in traffic scene based on boosted HOG features and SVM," in *Proc. IEEE 9th Int. Symp. Intell. Signal Process. (WISP)*, May 2015, pp. 1–4.
[31] Y. Feng, Y. Song, and Y. Zhang, "Scene text localization using extremal regions and corner-HOG feature," in *Proc. IEEE Int. Conf. Robot. Biomimetics (ROBIO)*, Dec. 2015, pp. 881–886.
[32] L. Mao, M. Xie, Y. Huang, and Y. Zhang, "Preceding vehicle detection using histograms of oriented gradients," in *Proc. Int. Conf. Commun., Circuits Syst. (ICCCAS)*, Jul. 2010, pp. 354–358.
[33] W. Jia, H. Zhang, and X. He, "Region-based license plate detection," *J. Netw. Comput. Appl.*, vol. 30, no. 4, pp. 1324–1333, Nov. 2007.
[34] Z.-Q. Zhao, P. Zheng, S.-T. Xu, and X. Wu, "Object detection with deep learning: A review," *IEEE Trans. Neural Netw. Learn. Syst.*, vol. 30, no. 11, pp. 3212–3232, Nov. 2019.
[35] Y. Wang, H. Yu, D. Sylvester, and P. Kong, "Energy efficient in-memory AES encryption based on nonvolatile domain-wall nanowire," in *Proc. Design, Autom. Test Eur. Conf. Exhib. (DATE)*, 2014, p. 183.
[36] T. Hastie, S. Rosset, J. Zhu, and H. Zou, "Multi-class AdaBoost," *Statist. Interface*, vol. 2, no. 3, pp. 349–360, 2009.
[37] D. E. Goldberg and J. H. Holland, "Genetic algorithms and machine learning," *Mach. Learn.*, vol. 3, nos. 2–3, pp. 95–99, 1988.
[38] G.-B. Huang, Q.-Y. Zhu, and C.-K. Siew, "Extreme learning machine: A new learning scheme of feedforward neural networks," in *Proc. IEEE Int. Joint Conf. Neural Netw.*, vol. 2, Jul. 2004, pp. 985–990.
[39] Y.-H. Pao and Y. Takefuji, "Functional-link net computing: Theory, system architecture, and functionalities," *Computer*, vol. 25, no. 5, pp. 76–79, May 1992.
[40] Y. Yang and Q. M. J. Wu, "Extreme learning machine with subnetwork hidden nodes for regression and classification," *IEEE Trans. Cybern.*, vol. 46, no. 12, pp. 2885–2898, Dec. 2016.
[41] D. Comaniciu and P. Meer, "Mean shift: A robust approach toward feature space analysis," *IEEE Trans. Pattern Anal. Mach. Intell.*, vol. 24, no. 5, pp. 603–619, May 2002.
[42] *EnglishLPDatabase-2001*. Accessed: Jul. 2016. [Online]. Available: http://www.zemris.fer.hr/projects/LicensePlates/english/
[43] *Online.Photo.Editor*. Accessed: Apr. 2017. [Online]. Available: https://www.freeonlinephotoeditor.com/
[44] K. S. Raghunandan, P. Shivakumara, H. A. Jalab, R. W. Ibrahim, G. H. Kumar, U. Pal, and T. Lu, "Riesz fractional based model for enhancing license plate detection and recognition," *IEEE Trans. Circuits Syst. Video Technol.*, vol. 28, no. 9, pp. 2276–2288, Sep. 2018.
[45] S. Azam and M. Gavrilova, "License plate image patch filtering using HOG descriptor and bio-inspired optimization," in *Proc. Comput. Graph. Int. Conf.*, Jun. 2017, pp. 1–6.
[46] F. Bashir and F. Porikli, "Performance evaluation of object detection and tracking systems," in *Proc. 9th IEEE Int. Workshop PETS*, Jun. 2006, pp. 7–14.
[47] D. François, "Binary classification performances measure cheat sheet," *J. Mach. Learn. Res.*, 2009. [Online]. Available: http://www.damienfrancois.be/blog/files/modelperfcheatsheet.pdf, doi: 10.1109/TAP.2013.2272673.
[48] A. Slaby, "ROC analysis with MATLAB," in *Proc. 29th Int. Conf. Inf. Technol. Interfaces*, Jun. 2007, pp. 191–196.
[49] A. Godil, R. Bostelman, W. Shackleford, T. Hong, and M. Shneier, "Performance metrics for evaluating object and human detection and tracking systems," Nat. Inst. Standards Technol., Gaithersburg, MD, USA, Tech. Rep. NISTIR 7972, 2014.
[50] B. B. Yousif, M. M. Ata, N. Fawzy, and M. Obaya, "Toward an optimized neutrosophic k-Means with genetic algorithm for automatic vehicle license plate recognition (ONKM-AVLPR)," *IEEE Access*, vol. 8, pp. 49285–49312, 2020.
[51] C. Henry, S. Y. Ahn, and S.-W. Lee, "Multinational license plate recognition using generalized character sequence detection," *IEEE Access*, vol. 8, pp. 35185–35199, 2020.

MEERAS SALMAN AL-SHEMARRY received the bachelor's degree in computer science from Babylon University, Iraq, in 2002, and the master's degree in IT from University Utara Malaysia (UUM), Malaysia, in 2010. She is currently pursuing the Ph.D. degree with the Faculty of Health, Engineering and Sciences, University of Southern Queensland, Australia. She is also a Lecturer with the Department of Computer, College of Science, Karbala University, Iraq. Her research interests include system analysis using UML diagrams, image processing and objects detection, artificial intelligence, and database management systems.

YAN LI is currently a Professor of computer science with the School of Sciences, University of Southern Queensland, Australia. Her research interests include artificial intelligence, big data analytics, signal and image processing, biomedical engineering, artificial intelligence, big data analytics, and computer networking technologies.